

Waterborne Cationomer Polyurethane Coatings with Improved Hydrophobic Properties

Piotr Król, Bożena Król, Ryszard Stagraczyński, Krzysztof Skrzypiec*

Department of Polymer Science, Faculty of Chemistry, Rzeszów University of Technology, Rzeszów, Poland

* Faculty of Chemistry, The Maria Curie-Skłodowska University, Plac M.C. Skłodowskiej 3, 20-031 Lublin, Poland

Correspondence to: P. Król (E-mail: pkrol@prz.edu.pl)

ABSTRACT: The AFM method was used to investigate the phase structure of the coatings, which have been obtained after application of polyurethane cationomers, synthesized in the reaction of 4,4'-methylenebis(phenyl isocyanate) or isophorone diisocyanate with polyoxyethylene glycol ($M = 600$) and *N*-methyl or *N*-butyldiethanolamine with 2,2,3,3-tetrafluoro-1,4-butanediol. Changes were discussed in the surface-free energy (SFE) and its components, as calculated independently according to the method suggested by van Owens–Wendt, in relation to chemical structures of cationomers, as well as morphology of coating surfaces obtained from those cationomers. Fluorine incorporated into cationomers (about 2–5%) contributed to lower SFE values, down to about 30 mJ/m². An attempt was made to use ¹H-NMR spectroscopy to provide more extensive grounds for the effect of polyurethane chemical structures (by parameters κ) on the SFE of coatings obtained from such polyurethanes, with the values of SFE (γ_s , γ_s^p) and determined by the Owens–Wendt method. © 2012 Wiley Periodicals, Inc. *J. Appl. Polym. Sci.* 000: 000–000, 2012

KEYWORDS: waterborne polyurethane cationomers; chemical structure; ¹H-, ¹³C- and ¹⁹F-NMR spectrometry; estimation of the polarity level; phase structure by AFM method

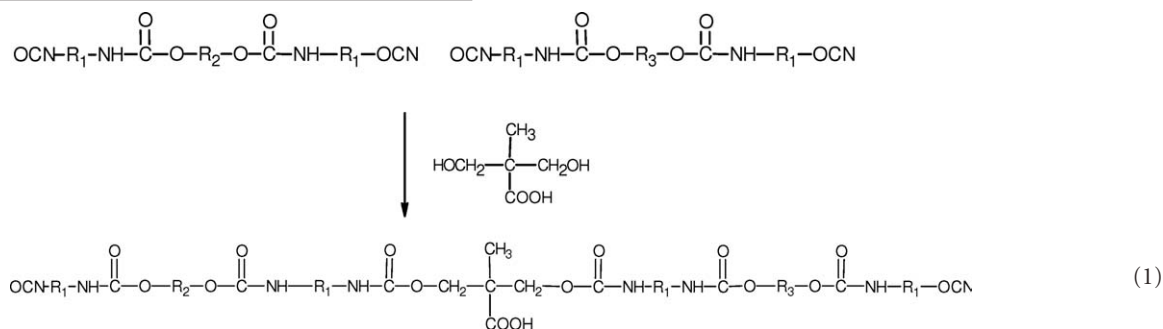
Received 28 March 2011; accepted 21 February 2012; published online

DOI: 10.1002/app.37552

INTRODUCTION

Waterborne polyurethane ionomers are defined as polymers, which contain small numbers of ionic groups (<10%) in their urethane-polymer backbones. These may be classified as anionomers or cationomers, depending on the type of

ionic groups, which have been built in. In case of anionomers, those groups are —COOH most frequently and they come, e.g., from 2,2-bis(hydroxymethyl)propionic acid, which has been built in into the urethane-isocyanate prepolymer^{1,2}:



where:

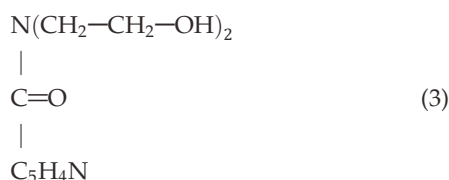
- R₁—structure derived from diisocyanate (MDI, TDI, HDI, or IPDI).
- R₂—structure derived from polyol (polyether or polyester).

Cationomers, on the other hand, contain tertiary nitrogen atoms in the backbone chains, which are derived, e.g., from *N*-alkyl diethanolamine^{3–5}



© 2012 Wiley Periodicals, Inc.

or *N,N'*-bis(2-hydroxyethyl)isonicotinamide:



These are used *inter alia* for the production of ionomer films with antibacterial performance.⁶ Polyurethane ionomers attract much interest since they may be used to prepare aqueous dispersions, which are then applicable as ecological waterborne polyurethane lacquers, adhesives, or latex thickeners.⁷ Polyurethane cationomers accept various cations, which can be incorporated into their structures (ammonium, sulfonium, or phosphonium cations) together with suitable counter-ions. Physicochemical interactions with acid–base nature, electrostatic interactions, interactions through hydrogen bonds, as well as polar and dispersity interactions can be improved in this method. Those effects are decisive *inter alia* for improved mechanical strength of polyurethane elastomers, permeability, and selectivity of polyurethane membranes, which are especially suitable for separation of organic mixtures by pervaporation and vapor permeation methods.⁸

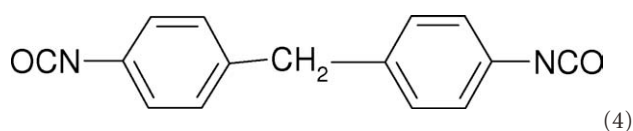
Attention was paid in our earlier studies to the extensive potential for modifications of surface properties of the polyurethane coatings, which are synthesized from polyurethane cationomers, which contain tertiary nitrogen atoms derived from *N*-alkyl or *N*-phenyl diethanolamines. The authors demonstrated the possibility of adjusting the hydrophobic properties of the polyurethane coatings by changing the type(s) of diisocyanate and quaternary ammonium groups, which are present in the polyurethane chain and which were derived from diethanolamines and formic acid or alkyl bromides. Our research has been focused on the relation between the structures of polyurethane cationomers and surface-free energy (SFE) values of polyurethane coatings.⁹ High values of SFE are of basic importance for adhesion of polyurethane coatings to wood, metals, and ceramics, but they are not favorable for chemical and biological resistance of those coatings.

The purpose of this article is to study the additional contribution of fluorine to the polyurethane structure and to the properties of polyurethane coatings, when synthesized from MDI or IPDI and *N*-methyl or *N*-butyl diethanolamine. Their SFE values were to be determined, either.

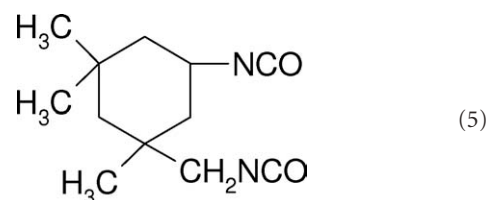
EXPERIMENTAL

Reagents

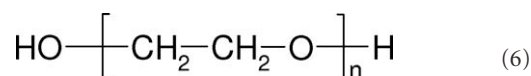
4,4'-Methylenebis(phenyl isocyanate; $M = 250.25$ g/mol) (MDI) from Aldrich. The reagent was used as purchased.



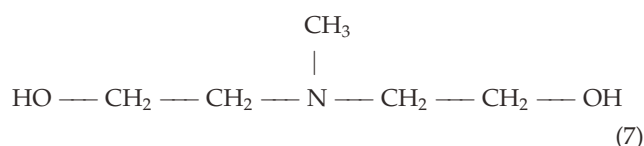
Isophorone diisocyanate [5-isocyanato-1-(isocyanatomethyl)-1,3,3-trimethylcyclo-hexane] (IPDI) from Aldrich. The reagent was used as purchased.



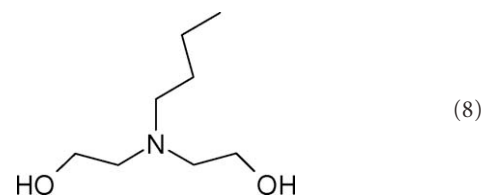
Polyoxyethylene glycol (PEG; $M_n = 570\text{--}630$ g/mol, Aldrich) in which product was dried under vacuum in nitrogen, at 120°C , during 2 h.



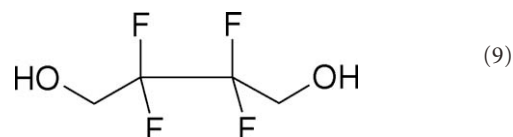
N-Methyl diethanolamine (*N*-MDA) (Aldrich).



N-Butyl diethanolamine (*N*-BDA), (Aldrich).



2,2,3,3-Tetrafluoro-1,4-butanediol (TFBD) from Aldrich. The reagent was used as purchased.



1,6-Hexamethylenediamine (HMDA) from Aldrich. The reagent was used as purchased.



Dibutyl tin dilaurate (DBTL; from Huntsman Performance Chemicals).

Tetrahydrofuran (THF; from POCh S.A., Gliwice, Poland).

Formic acid (HCOOH), 99%, analytically pure (POCh S.A., Gliwice, Poland).

Table 1. Synthesized Cationomer Coatings

Sample no.	Synthesis of type BAB isocyanate prepolymer				First propagation		Quaternization agent		Dispergation and second propagation agent		Fluorine content in cationomer (wt %)	Surface roughness	
	Stage 1		Stage 2		Stage 3	Stage 4	Stage 3	Stage 4	Stage 3	Stage 4		R _{ca} (μm)	R _{z1} (μm)
	Type of diisocyanate (B)	Type of polyol (A)	Dihydroxylamine	Dihydroxylamine (X)									
1	MDI	PEG 600	N-MDA	N-MDA	N-MDA	HCOOH	HMDA	0	0.010	0.10			
2	MDI		N-MDA + 5 wt % TFBD	N-MDA + 5 wt % TFBD	N-MDA + 5 wt % TFBD			0.54	0.018	0.15			
3	MDI		N-MDA + 10 wt % TFBD	N-MDA + 10 wt % TFBD	N-MDA + 10 wt % TFBD			1.09	0.020	0.18			
4	MDI		N-MDA + 15 wt % TFBD	N-MDA + 15 wt % TFBD	N-MDA + 15 wt % TFBD			1.66	0.024	0.24			
5	IPDI		N-MDA	N-MDA	N-MDA			0	Not analyzed				
6	IPDI		N-MDA + 5 wt % TFBD	N-MDA + 5 wt % TFBD	N-MDA + 5 wt % TFBD			0.55					
7	IPDI		N-MDA + 10 wt % TFBD	N-MDA + 10 wt % TFBD	N-MDA + 10 wt % TFBD			1.09					
8	IPDI		N-MDA + 15 wt % TFBD	N-MDA + 15 wt % TFBD	N-MDA + 15 wt % TFBD			1.79					
9	MDI		N-BDA	N-BDA	N-BDA			0	0.023	0.15			
10	MDI		N-BDA + 5 wt % TFBD	N-BDA + 5 wt % TFBD	N-BDA + 5 wt % TFBD			0.68	0.027	0.17			
11	MDI		N-BDA + 10 wt % TFBD	N-BDA + 10 wt % TFBD	N-BDA + 10 wt % TFBD			1.36	0.038	0.21			
12	MDI		N-BDA + 15 wt % TFBD	N-BDA + 15 wt % TFBD	N-BDA + 15 wt % TFBD			2.04	0.059	0.29			

The factor κ was calculated as follows:

$$\kappa = \frac{I_P}{I_P + I_N} \cdot 100\% \quad (14)$$

where:

$$I_P = \sum I_{P_n} = 0.5 (I_b + I_{b'}) + I_c + I_e + I_u + I_m + I_x + I_q + I_y \quad (15)$$

$$I_N = \sum I_{N_n} = 0.5 (I_b + I_{b'}) + I_w + I_c + I_d + I_a + I_g + I_i + I_j + I_k + I_l \quad (16)$$

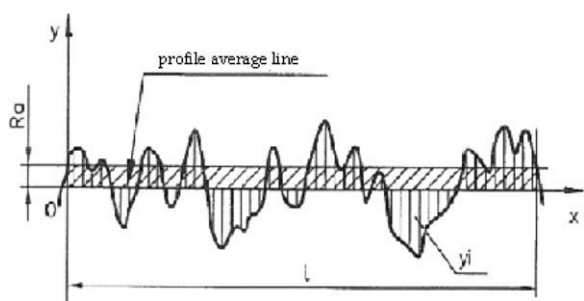
For simplification, the authors assume that $\text{CH}_2\text{-O}$ (b) and $\text{CH}_2\text{-N}$ (b') groups have equivalent contributions to polar and nonpolar interaction.

Surface Roughness

The surface roughness grade of the synthesized coatings was determined by means of the MarSurf PS1 apparatus (from Mahr). The following parameters were measured to describe the surface roughness grade of the obtained coats.¹¹

R_a —arithmetic mean of the absolute values for y deviations of the profile from the average line n , over the elementary length l :

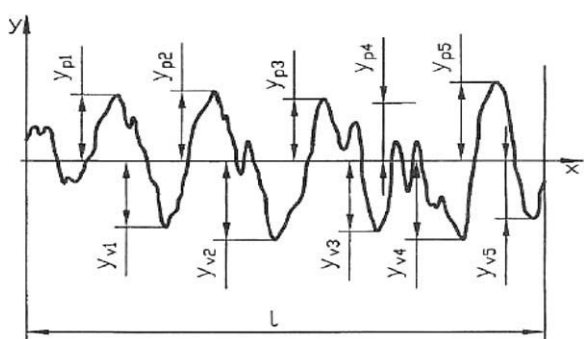
$$R_a = \frac{1}{n} \sum_{i=1}^n |y_i| \quad (17)$$



(18)

R_z —arithmetic mean of the absolute values for five highest peaks in the roughness profile (y_{pi}) and five deepest pits in the roughness profile (y_{vi}), over the elementary length l :

$$R_z = \frac{1}{5} \left(\sum_{i=1}^5 |y_{pi}| + \sum_{i=1}^5 |y_{vi}| \right) \quad (19)$$



(20)

Table II. Surface Properties of Model Measuring Liquids¹⁴

Model measuring liquid	Surface-free energy parameters (mJ/m ²)		
	γ_L	γ_L^d	γ_L^p
Water	72.8	21.8	51
Formamide	58	39	19
Diiodomethane	50.8	48.5	2.3

Microscopic Analysis

The structural analysis of the surfaces of the cationomer coats was performed with the use of an optical microscope Nikon Eclipse LV100POL, with no polarization, in the transmitted light.

Atomic Force Microscopy

The atomic force microscope (Nanoscope III, Digital Instrument, USA) was used to study superficial structures of the coating obtained from FP. The scans were taken at ambient temperature, in air, and at *tapping mode* (TM) conditions, i.e., at the direct contact between the sample surface and the tip. The pyramidal Si tip used in the TM system had a spring constant of 20–80 N/m (NanoprobeTM). Each scan was presented in the following data formats:

- topographic image (height, h), two-dimensional or three-dimensional (3d)
- phase image (phase, p), which represented the phase lag for probe vibrations at the boundary between two media (due to friction of the probe/needle tip on the sample surface (friction, f) or axial deflection z of the probe/needle tip after it hits any surface irregularity (deflection, d).

Method for Determination of Components of Surface-Free Energy for Solids

Physical parameters of the surface energy of a solid γ_S were found on the basis of the Owens–Wendt method. The van Owens–Wendt model assumes that the SFE $\gamma_{S,L}$ may be presented as a sum of two components^{12,13}:

$$\gamma_{S,L} = \gamma_{S,L}^d + \gamma_{S,L}^p \quad (21)$$

where $\gamma_{S,L}^d$ —surface energy connected with dispersion interactions; $\gamma_{S,L}^p$ —surface energy connected with polar acid–base interactions.

Equation (21) is generally applicable both to a solid phase, and the subscript of S is used then, and to a wetting liquid (standard liquid or tested liquid), with the subscript of L. The Owens–Wendt method was also convenient to authors since it made it possible to evaluate the share of polar interactions in the total value of SEP, and thus it was possible to refer the values obtained for γ_S to the “amounts” of polar structures in produced cationomers (κ) as estimated from NMR spectra [eq. (14)].

The SFE parameters for solids (S) and for liquids (L) interacting with those solids had to satisfy the Owens–Wendt equation:

$$\gamma_L \cdot \frac{1 + \cos \Theta}{2} = \sqrt{\gamma_S^d \cdot \gamma_L^d} + \sqrt{\gamma_S^p \cdot \gamma_L^p} \quad (22)$$

Table III. Experimental Values of Contact Angles and Parameters of SFE as Calculated by van Owens–Wendt Method for Cationomer Coatings

Sample no. (by Table I)	Experimental values of contact angles Θ (°)			Parameters of SFE (mJ/m ²)					
	Model liquids			Formamide–diiodomethane			Water–diiodomethane		
	Water	Formamide	Diiodomethane	γ_s^d	γ_s^p	γ_s	γ_s^d	γ_s^p	γ_s
1	56.5	32.9	29.9	36.29	13.04	49.33	35.21	16.24	51.44
2	81.4	54.4	44.2	33.29	5.09	38.38	33.80	4.234	38.03
3	84.0	57.7	51.7	28.71	6.424	35.13	29.830	4.24	34.07
4	99.0	63.4	59.1	24.80	6.224	31.02	31.95	0.36	32.31
5	61.2	35.2	28.2	37.80	10.764	48.56	37.010	12.79	49.80
6	70.8	40.0	31.0	37.51	8.864	46.37	38.16	7.479	45.63
7	80.5	46.9	34.8	37.321	6.00	43.32	38.91	3.45	43.36
8	84.1	58.9	36.1	40.831	0.87	41.71	39.21	2.32	41.53
9	80.5	63.4	45.4	35.72	1.14	36.86	32.89	4.78	37.67
10	86.9	75.9	50.4	35.48	$4 \cdot 10^{-4}$	35.48	31.02	3.02	34.03
11	101.2	75.4	59.9	28.31	0.499	28.80	28.51	0.38	28.89
12	108.0	81.0	62.5	28.27	$6 \cdot 10^{-3}$	28.27	28.35	<0.10	28.35

where Θ is the experimentally found contact angle between a liquid drop and a solid surface under investigation. So, contact angles Θ were first measured for the surfaces of cationomer coatings with the use of two pairs of model liquids (water–diiodomethane and formamide–diiodomethane) with on margin known parameters of γ_L , γ_L^d , and γ_L^p (Table II).¹⁴ Then, eq. (22) was used to calculate the values of γ_S^d and γ_S^p for the studied cationomers. The values of γ_S were calculated from eq. (21).

The contact angles Θ were measured with the use of the method suggested by Zisman,¹⁵ i.e., by means of an optical goniometer (*Cobrabid Optica*—Warsaw) with a digital camera installed in the axial direction of its lens. The liquid drops with the constant volume (about 3–5 μdm^3) were applied to the surfaces of the studied samples with the use of a special micropipette. The samples were fixed on the stage of the goniometer. The measurements were taken at $21 \pm 1^\circ\text{C}$. The values of contact angles were found from the geometric analysis of pictures taken for liquid drops, which involved the use of our originally developed software *Kropka* for interpretation of the Young's equation. The measuring errors for angles Θ come from two sources. The first of them results from different shapes of liquid drops placed on the investigated coatings, and from possible interactions between the standard liquid and that substrate, as well as from different liquid vaporization rates observed when the pictures were taken. Nine drops were analyzed each time, which were placed on the surface simultaneously. Another source of potential errors is inaccuracy in graphical interpretation of the pictures with the use of the computer software. For each picture recorded (i.e., for each liquid drop), the geometrical shape analysis was repeated 10 times: the extreme values were rejected and the arithmetic mean value was calculated for the accepted findings. The measured values of contact angles and the components of the SFE for the cationomer coatings as derived from those measurements were presented in Table III.

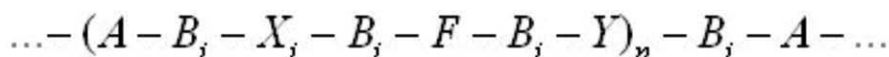
RESULTS AND DISCUSSION

Chemical Structure of Cationomers

The structures of backbone chains of resulting cationomers are presented in Figure 1. The protons in these structures were indicated by letters and carbon atoms—by numbers. The additional information about the synthesized polyurethanes was provided in Table I.

The chemical structures of the synthesized cationomers were verified on the basis of the ¹H- and ¹³C-NMR spectra.^{16,17} By the method of example, Figure 2 presents the ¹H spectrum and Figure 3—¹³C-NMR spectrum for the cationomer no. 9. After analyzing the signals in ¹H and ¹³C spectra, one can infer that the produced cationomers had different chemical compositions, despite the same reaction stoichiometry assumed for corresponding process stages. That could be explained by the presence of different chemical species (i.e., oligomers) in the process, by different reactivity specifications of —NCO groups in diisocyanate isophorone and in the prepolymer intermediate products, etc. Moreover, prepolymer extension reactions with HMDA under aqueous dispersion conditions occurred with different yields. Our analysis was limited in this article to NMR spectra for cationomers, which did not contain fluorine (Samples no. 1, 5, and 8) or contained the highest fluorine shares (Samples no. 4, 8, and 12), to make that analysis easier to understand.

All fluorine atoms were recorded in the ¹⁹F-NMR spectrum of the monomer TFBD as a singlet located within $\delta = -123.24/-123.31$ ppm, while a triplet could be noticed in the ¹H-NMR spectrum of that compound, which was specific for groups —CH₂—OH (at $\delta = 3.84$ ppm) and a singlet for groups —OH (at $\delta = 5.73$ ppm). In the case of cationomer 12, however, the ¹⁹F-NMR spectrum demonstrated three groups of signals: $-120.93/-120.99$; $-121.33/-121.57$, and $-122.74/-122.93$ ppm.



where: $i = 1, 2$

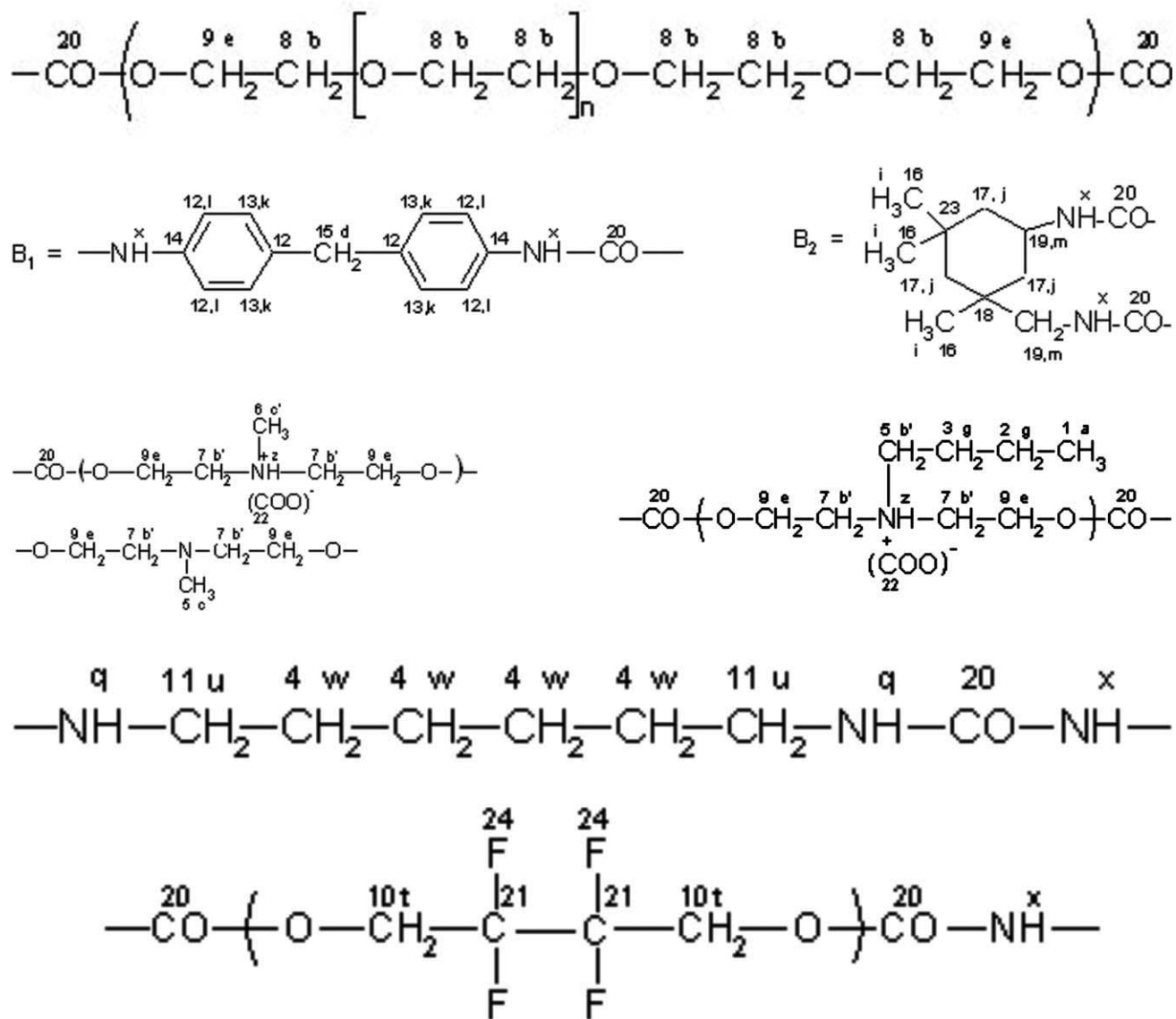


Figure 1. Structures of polyurethane chains in the synthesized cationomers.

The signals at $\delta = 3.84$ and at 5.73 ppm could no longer be observed in $^1\text{H-NMR}$ spectra for cationomers no. 4 and 12. Hence, when the $^1\text{H-}$ and $^{19}\text{F-NMR}$ spectra for the monomer TFBD and for the cationomers synthesized with the use of that monomer were compared thoroughly, the authors arrived at the conclusion that the monomer TFBD had been incorporated into cationomer chains, which contained fluorine.

The values of κ as calculated from $^1\text{H-NMR}$ spectra (Figure 8) decrease within $\kappa = 60$ to 37% for cationomers no. 1 and 5, which were synthesized from MDI and *N*-MDA based IPDI, and within $\kappa = 60$ to 32% for cationomers no. 1 and 9, which were synthesized from *N*-MDA and *N*-BDA based MDI. When

analyzing those changes in the values for the factor κ , one had to pay attention to the fact that those changes are well-representative for reduced polarity of cationomers when the diisocyanate feed is changed from MDI to IPDI, and when *N*-MDA is substituted with *N*-BDA.

Surface Shape and Morphology of Studied Coats

Having in mind that the coatings will then be used to measure the wetting angles, which is necessary to calculate the SFE values, it was essential to study the geometric shapes (profiles) and morphology of the surfaces of some cationomer samples, which were selected for further investigation. When wetting angles are measured, the critical role is played by the surface roughness,

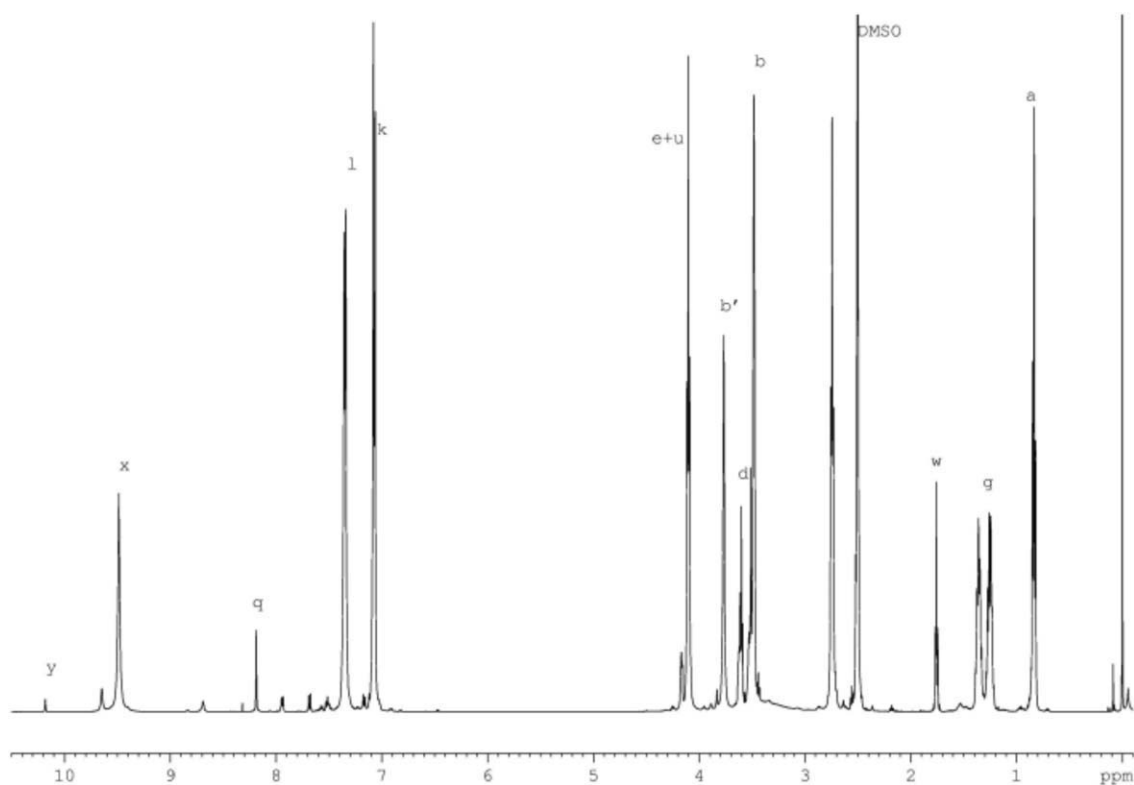


Figure 2. ^1H -NMR spectrum for cationomer no. 9, synthesized with the use of MDI diisocyanate prepolymer, PEG, *N*-BDA, quaternization by HCOOH .

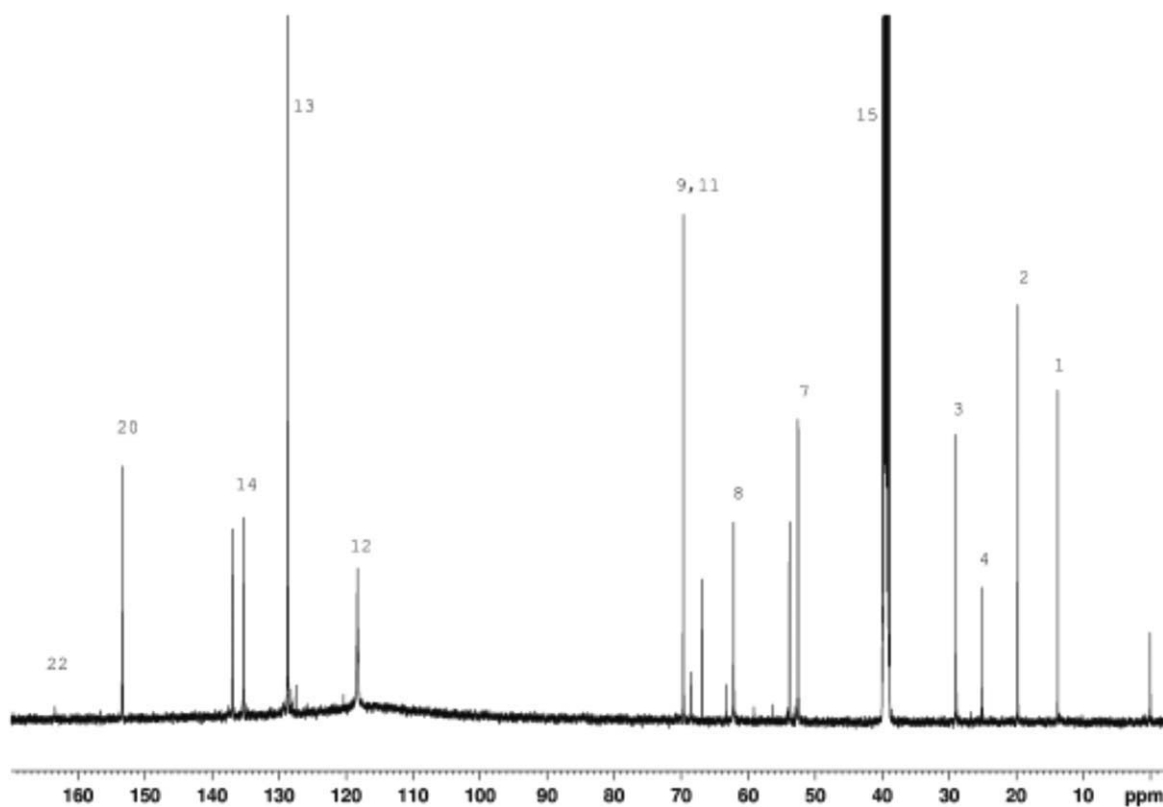


Figure 3. ^{13}C -NMR spectrum for cationomer no. 9, synthesized with the use of MDI diisocyanate prepolymer, PEG, *N*-BDA, quaternization by HCOOH .

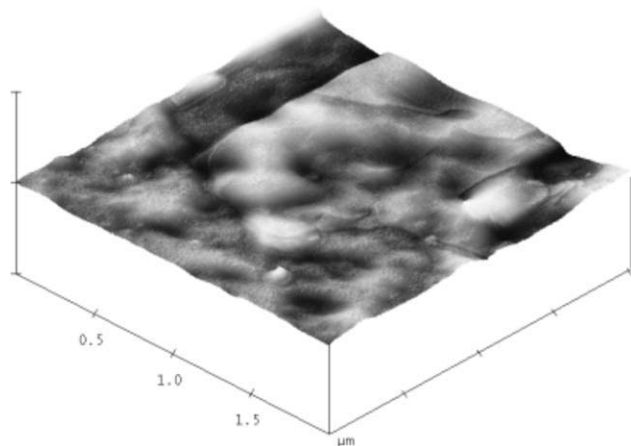


Figure 4. 3D AFM $2\ \mu\text{m} \times 2\ \mu\text{m}$ image for cationomer no. 1, obtained by the “moderate tapping” method.

which is decisive for the geometric shape of a liquid drop at the solid–liquid interphase. That factor is directly determining for the question whether a wetting angle can be properly measured by means of an optical goniometer or not. Table I provides geometric parameters R_a and R_z , which are specific for the assessment of the surface roughness, and which go up to follow the increasing amounts of fluorine incorporated in cationomers. A question had to be asked in this article, whether the observed increase results only from the method, in which, a cationomer dispersion was applied to the PTFE surface, or whether it may also result from the morphological features of the surface, which assumes spontaneously some surface shapes, when it dries out. The authors were convinced that the dominating effect resulted from the presence of fluorine. To find the answer, more detailed investigations with the use of AFM and optical microscopy methods were conducted.

The AFM analyses show that the superficial structures of the coats are generally inhomogeneous, which results from limited miscibility of hard and soft segments. The system comprises lots of various rigid segments, and they are derived from urethane structures in diisocyanates, from urea, from the chain extension agent (HMDA) and from polar structures of quaternary amino groups (in *N*-MDA or *N*-BDA), and from the counter-ion supplied by HCOOH. That is clearly visible in Figure 4, i.e., in the three-dimensional AFM image of the fluorine-free cationomer surface. Urethane segments, coming from diisocyanate and TFBD, are definitely less polar, hence they may appear at the border between the rigid and flexible phases, which contributes to phase homogenization, as confirmed by AFM images presented in Figure 5 for cationomers, which contain 10% TFBD in their soft segments. However, “islands” of hard segments with sharply outlined shapes are visible even in those samples against the background of the pretty homogeneous phase composed of soft segments.

A similar effect, although not so clear, was recorded in two-dimensional images, type height, and phase, which is clearly apparent in Figure 6, which present topographic and phase images for cationomer coatings no. 2. Thus, even insignificant

amounts of fluorine yield microscopically more homogeneous coatings, in which, however hard segments distinctly tend to agglomerate into small and compact zones. That can be the explanation for the increased surface roughness of coatings—as observed macroscopically. A similar problem was analyzed by Young et al.¹⁸ Surface morphology was studied there for a coat obtained after evaporation of water from the mixture of polyurethane anionomer (derived from HMDI, PTMO, and dimethylolbutanoic acid) and urethane oligomer (prepared with the use of a fluorine reagent: Zonyl BA-N ($\text{F}(\text{CF}_2)_{10}\text{CH}_2\text{CH}_2\text{OH}$, DuPont) as the fluoroalkyl alcohol). The authors found out that fluorine-containing hard segments offered a more crystalline nature and they tended to migrate toward the surface, to contribute to improved hardness and mechanical strength of the polymer film, and to its definitely higher hydrophobicity.

Inhomogeneity of a fluorinated cationomer, and its better phase arrangement at the same time, can also be observed in the pictures, which were taken by means of a Nikon Eclipse optical microscope. Figure 7 provides microscopic images for coatings of cationomers no. 9 and 12, which were synthesized from MDI and *N*-BDA. Light-colored and dark-colored areas stand out against the fluorine-modified cationomer surface in that picture. The light-colored ones probably represent fluorine-containing segments, while the dark-colored ones make fluorine-free soft segments. Reference can be made in this article to the report¹⁹ where the effect of fluorine was tested on morphology of the hard phase, which was formed in the aliphatic polyurethanes, which were synthesized from either hexamethylene diisocyanate (HDI) and 2,2,3,3-tetrafluoro-1,4-butanediol or HDI and 1,4-butanediol. The crystallization behaviors of those polyurethanes were characterized using differential scanning calorimetry, wide-angle X-ray diffraction, and polarized optical microscopy. The fluorinated polyurethanes were found to exhibit lower viscosity, higher solubility in organic solvents, smaller fraction of ordered hydrogen-bonded carbonyls, and lower transition temperatures than the corresponding fluorine-free polyurethanes. The wide-angle X-ray diffraction measurements reflected changes in the crystal structure with the $(\text{CF}_2)_2$ moieties in place of $(\text{CH}_2)_2$

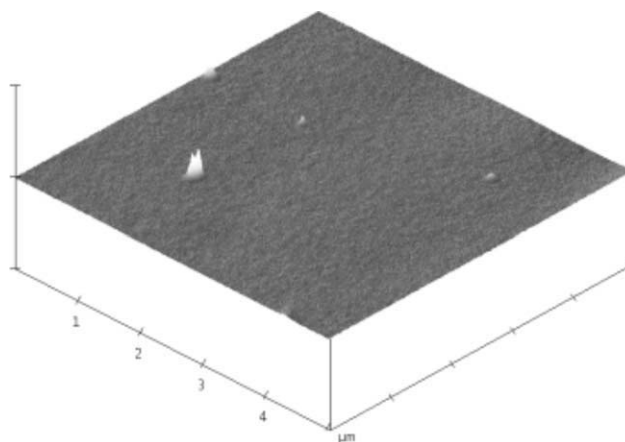


Figure 5. 3D AFM $5\ \mu\text{m} \times 5\ \mu\text{m}$ image for cationomer no. 3, obtained by the “moderate tapping” method.

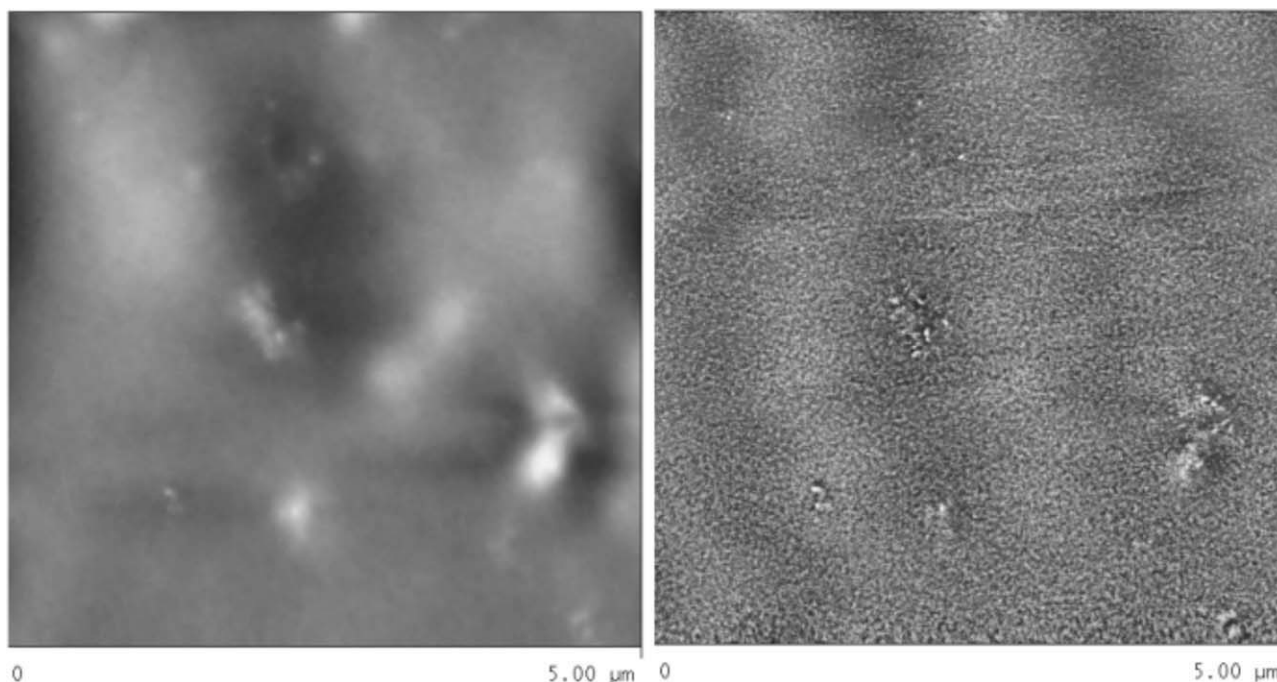


Figure 6. Topographic (left-hand side) and phase (right-hand side) AFM $5\ \mu\text{m} \times 5\ \mu\text{m}$ images for cationomer no. 2, obtained by the “moderate tapping” method.

moieties. The polarized optical microscopy also revealed that the polyurethanes exhibited different spherulitic textures.¹⁹ Thus, the presence of fluorine undoubtedly affects morphology and ability of polyurethanes to crystallize, and it generally reduces intermolecular interactions in polyurethanes, which had to be reflected in their lower SFE values. Yet, one can hardly explain the noted increase in surface roughness of the synthesized coats solely by migration of still amorphous, fluorinated hard segments toward the coating surface.

Surface-Free Energy of Coatings Obtained from Polyurethane Cationomers

Table III presents the wetting angle values Θ and the component values γ_S^d and γ_S^p as calculated from those angles. The comparative analysis of the finding for two sets of standard liquids used: water–diiodomethane and formamide–diiodomethane, made it possible to authenticate those results. The data reveal that the highest value of SFE, i.e., about $50\ \text{mJ}/\text{m}^2$, is available for the coat no. 1, which was produced with the use of

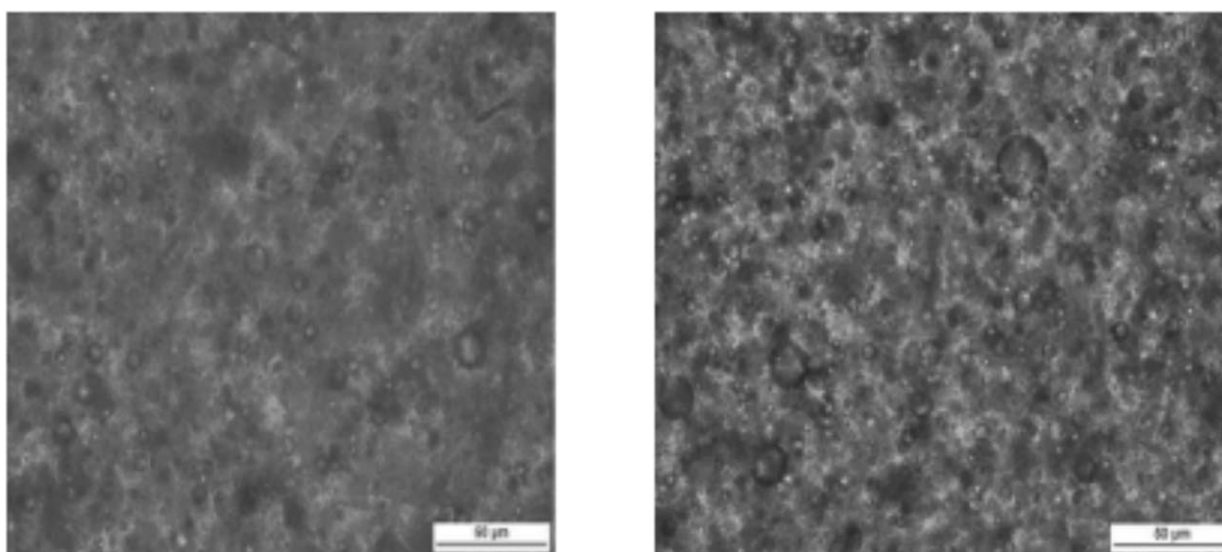


Figure 7. Images for the coatings obtained from cationomer no. 9 (left-hand side) and no. 12 (right-hand side) as recorded under the *Nikon Eclipse LV100POL* optical microscope.

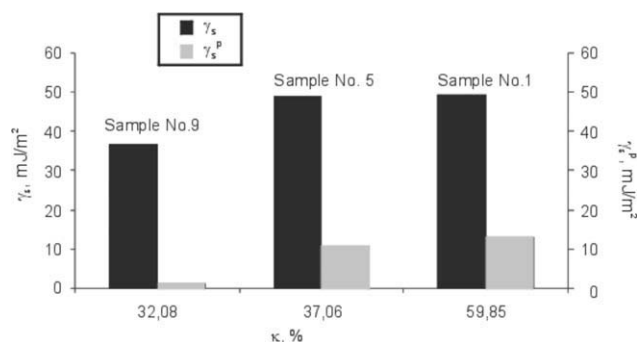


Figure 8. Relations between the experimental values of the SFE (γ_s), polar components (γ_s^p) and parameters κ calculated from ^1H NMR spectra of synthesized polyurethane cationomer coatings without fluoride in polymer chains.

MDI and *N*-MDA. When, in the cationomer which contains no fluorine, IPDI (sample no. 5) is used as the isocyanate substrate instead of MDI (sample no. 1), the SFE values will undergo slight lowering only, from 49.3 down to 48.6 mJ/m^2 . Incorporation of fluorine, however, to the cationomers prepared with the use of MDI clearly reduces SFE: from 49 down to 31 mJ/m^2 . For cationomers obtained from IPDI with the addition of fluorine, reduction of SEP is also considerable, from 46.4 (sample no. 6) down to 41.7 mJ/m^2 (sample no. 8). If additionally *N*-MDA is replaced by a more hydrophobic amine, *N*-BDA, then SEP of the cationomeric coats prepared with the use of MDI suffers further reduction to the value of 36.9 mJ/m^2 (sample no. 9), and when fluorine is additionally present—even down to 28.3 mJ/m^2 (sample no. 12).

It had to be kept in mind that the SFE value below 30 mJ/m^2 for a coating makes a proof for clearly hydrophobic performance of that coating, which is typical, e.g., for polypropylene.¹⁴ Such SFE values were recorded for cationomers no. 11 and 12, which were synthesized from MDI and *N*-BDA.

It had to be stressed clearly in this article that the decrease of the SFE by incorporation of the fluorine component had to be attributed to not only the hydrophobicity of that component but also to the migration of fluorine to the surface layer during the formation of the coating film. Therefore, the determination of the F/C ratio by ESCA with the fluorine content can support the grounds of significant decrease of SFE and phase separation, which may cause the surface roughness. Special sample pretreatment is needed, however, for such measurements.

An interesting question emerges when the experimental values of γ_s are compared with the factor κ values as calculated from ^1H -NMR spectra. Relations between the experimental values of the SFE parameter (γ_s) and those of the parameter κ , which makes it possible to compare polarities of synthesized cationomers, and which is calculated from ^1H NMR spectra, were shown in Figure 8. As results from that figure, there is the same correlation between the analyzed quantities for the polymers with similar chemical structure-free from fluorine atoms. Especially, valuable for the κ factor definition is the observed relation between the γ_s^p components for cationomers no. 1, 5, and 9, as determined using the Owens–Wendt method and the κ

factors calculated on the basis of the ^1H -NMR spectra. The values of γ_s^p for all observed coatings are much lower than those for γ_s^d , which suggests that dispersion interactions are dominant interactions in the studied cationomers. The SEM and microscopic studies demonstrated that the presence of F atoms changed to some extent the surface morphology, and that could also influence the values of SFE. That is why, in our opinion, the values of γ_s did not follow regularly the increasing amounts of built-in fluorine. In that situation, one may consider the additional effects of the dispersion interactions, which are represented by the dispersion component γ_s^d of SFE.

CONCLUSION

Polyurethane cationomers offer a considerable potential for structural modifications, which are aimed at obtaining some desired performance properties of elastomers and coatings. In the form of waterborne lacquers, moreover, they are more environmentally friendly when applied as protective coatings. It is essential for some applications to improve the hydrophobic performance of polyurethane coatings, which are generally hydrophilic.

As a result from our research, the question of decreasing polarity of polyurethanes must be analyzed with due consideration of chemical structures of polymer chains. After the above issues have been considered, it is possible to lower the SFE values of polyurethanes within from 50 down to 30 mJ/m^2 by changes in polymer chain chemical structures and by incorporation of segments, which will reduce polar interactions, i.e., in particular, replacements within diisocyanates, e.g., substitution of MDI by less polar IPDI, and by the use of more hydrophobic tertiary amines, which produce amino groups, e.g., *N*-butyldiethanolamine instead of *N*-methyldiethanolamine. The highest reduction in SFE, however, was obtained by the use of *N*-alkyldiethanolamine with small admixtures of 2,2,3,3-tetrafluoro-1,4-butanediol, which combined with PEG and produced new soft segments. High diversity of reagents, which were added at successive stages of the synthesis process, together with the complex process which yielded aqueous dispersions, and the assumed coat application process, all that produced structures with different degrees of arrangement and clearly noticeable separation of phases, i.e., soft and hard segments within the cationomer structures. The essential change in SFE of fluorine-containing coats may be supposed to result from migration of less polar soft segments, with incorporated 2,2,3,3-tetrafluoro-1,4-butanediol, toward the coating surface. Especially, valuable is the stated correlation between the γ_s^p component for cationomers no. 1, 5, and 9 without fluorine and κ factors from ^1H -NMR as determined with the use of the Owens–Wendt method.

ACKNOWLEDGMENTS

This work has been supported by the Polish Ministry of Science and Higher Education under contract No. N N507 329636.

REFERENCES

1. Robilà, G.; Buruianà, T.; Buruianà, E. C. *Eur. Polym. J.* **1999**, *35*, 1305.
2. D'Ilario, F. L.; Guaglianone, E.; Donelli, G.; Martinelli, A.; Piozzi, A. *Acta. Biomater.* **2010**, *6*, 3482.

3. Jeong, E. H.; Yang, J.; Youk, J. H. *Mater. Lett.* **2007**, *61*, 3991.
4. Kébir, N.; Campistron, I.; Laguerre, A.; Pilard, J. F.; Bunel, C. *Biomaterials* **2007**, *28*, 4200.
5. Król, P. Linear Polyurethanes; Koninklijke Brill NV: Leiden, **2008**.
6. Zhu, K.; Hu, J.; Yeung, K. *Acta. Biomater.* **2009**, *5*, 3346.
7. Sundar, S.; Arua, P.; Venkateshwardu, U.; Radhakrishnan, G. *Coll. Polym. Sci.* **2004**, *283*, 209.
8. Awkal, M.; Jonquires, A.; Clement, R.; Lochon P. *Polymer* **2006**, *47*, 5724.
9. Król, P.; Król, B. *Coll. Polym. Sci.* **2008**, *286*, 1111.
10. Stagg, F. E. *Analyst* **1966**, *71*, 557.
11. EN ISO **1997**, **12085**.
12. Żenkiewicz, M. *Polimery* **2006**, *51*, 169 and 584.
13. Owens, D. K.; Wendt, R. C. *J. Appl. Polym. Sci.* **1969**, *13*, 1741.
14. Chibowski, E.; Terpilowski, K. *Appl. Surf. Sci.* **2009**, *256*, 1573.
15. Zisman, W. A. *Ad. Chem. Am. Chem. Soc.* **1964**, *43*, 1.
16. Pham, Q. T. Proton and Carbon NMR Spectra of Polymers; John Wiley & Sons Inc.: Chichester, **2003**.
17. Lapprad, A.; Boisson, F.; Delolme, F.; Mèchin, F.; Pascault, J.-P. *Polym. Degrad. Stab.* **2005**, *90*, 363.
18. Young, H.; Min, J.; Lee, H.; Kim, B. K. *Coll. Surf. A Physico-chem. Eng. Aspects* **2006**, *290*, 178.
19. Chen, K.-Yu.; Kuo, J.-F. *J. Appl. Polym. Sci.* **2009**, *111*, 371.